CHAPTER IV

OSCILLATORY SHEAR INDUCED DROPLET DEFORMATION AND BREAKUP IN IMMISCIBLE POLYMER BLENDS

Vitsarut Janpaen

The Petroleum and Petrochemical College, Chulalongkorn University, Thailand.
Email: Rujzarus@gmail.com

Anuvat Sirivat

The Petroleum and Petrochemical College, Chulalongkorn University, Thailand.
Email: anuvat.s@chula.ac.th

Ronald G. Larson

The Department of Chemical Engineering, University of Michigan, Ann Arbor, Michigan, U.S.A.
Email: rlarson@engin.umich.edu

Alexander M. Jamieson

The Department of Macromolecular Science, Case Western Reserve University, Ohio, U.S.A.
Email: amj@po.cwru.edu

Synopsis

Droplets in polybutadiene/polydimethylsiloxane blends under oscillatory shear flow were observed using an optical flow cell. The apparent major axes, the minor axes, and the deformation of the droplets were measured from the time series of images. These deformation parameters were measured as functions of time, strain, frequency, G' ratios, and G" ratios. From the time series of the deformation parameters, it was possible to define deformation amplitudes, as the difference between the maximum and minimum values divided by two. The amplitudes of the deformation parameters increased linearly at small capillary number and nonlinearly at large capillary number, where the capillary is defined as the ratio between the viscous force and the interfacial tension force. The deformation parameters generally decreased with increasing viscosity ratio at a fixed capillary number. The amplitudes also decreased with increasing time scale ratio which is defined as the time scale ratio between the droplet relaxation time

scale and the oscillatory time scale. Drop breakup patterns observed depended critically on the time scale ratio.

I. INTRODUCTION

Properties of immiscible blends do not depend only on the properties of their components alone but also depend on the minor-phase morphology. Drop size, shape and size distribution resulting from mixing process can influence the final properties of the blend. The final morphology is controlled by the physicochemical and rheological properties of constitutional polymers, as well as the processing conditions. A better understanding of the relation between the morphology and the properties is required to predict the blend final product morphology.

The deformation and breakup of a suspended immiscible Newtonian droplet in another Newtonian matrix in a steady state shear flow was first pioneered and studied by Taylor (1932, 1934). He suggested that the droplet deformation is controlled by two dimensionless numbers: the viscosity ratio, η_r which is the ratio between viscosity of droplet (disperse phase) (η_d) and viscosity of matrix (η_m), and the Capillary number (Ca) or Taylor number, defined by the viscous force to the interfacial surface force:

$$Ca = \frac{\gamma \eta_m D_0}{2\Gamma} \tag{1}$$

where γ is the shear rate, D_0 is initial droplet diameter and Γ is interfacial tension. For small deformation, the shape of droplet gradually becomes ellipsoidal while its deformation, written as a function of its lengths, is given by:

$$Def \equiv \frac{a-b}{a+b} = Ca \frac{19\eta_r + 16}{16\eta_r + 16} \tag{2}$$

where a and b are the lengths of the major and minor axes of the deformed droplet (ellipsoidal shape), respectively. Taylor predicted that the critical point at which the viscous force overcomes the interfacial force leading to droplet breakup occurs at Ca_c

(critical capillary number) ≈ 0.5 and $\mathrm{Def_c}$ (critical deformation) ≈ 0.5 for a steady simple shearing flow (or quasi-steady), if the flow rate is very slowly increased with a viscosity ratio of around unity. Here, the word critical means the condition at breakup. These basic predictions have been confirmed by many experiments (Rumscheid and Mason 1961; Grace 1982; Bentley and Leal 1986; Guido and Villone 1997). When the viscosity ratio is higher than four, no breakup occurs (Grace (1982)). These results show that for Newtonian fluids, droplet deformation and breakup are strongly influenced by viscosity ratio. Grace (1982) found that, for steady state shearing of an isolated Newtonian droplet in a Newtonian matrix, the minimum critical capillary number occurs when the viscosity ratio is around unity.

The breakup of isolated viscoelastic drops in a Newtonian matrix and of Newtonian drops in a viscoelastic matrix in simple shear flow was investigated by Elmendorp and Maalcke (1985) with particular emphasis on the effect of elasticity. Their results showed that the droplets, which have higher elasticity, have more ability to resist against breakup because they tend to stabilize themselves. In contrast, the deformation of a Newtonian drop in a viscoelastic matrix increases with increasing matrix elasticity.

Mighri *et al.* (1998) investigated the influence of elastic properties on drop deformation and breakup in shear flow. They defined the elasticity ratio, k', as ratio of characteristic elastic time (λ) of the droplet phase to the matrix phase, where $\lambda = N_{1i}/2\eta\gamma^2$ and N_{1i} is the first normal stress difference. Their results show different mechanisms of the drop deformation between the elastic system and the Newtonian system of approximately the same viscosity ratio and the same interfacial tension. The steady-state drop deformation for shear rate less than critical value is affected by both the drop and matrix elasticities. The matrix elasticity helps to deform the drop, whereas the drop elasticity resists the drop deformation. For high elasticity (k'< 0.37) the deformation of elastic drops in an elastic matrix under shear is higher than that of Newtonian drops in a Newtonian matrix. However, for k' > 0.37, the elastic drops deform less than Newtonian drops in a Newtonian matrix. Thus, the droplet resistance

to deformation and breakup increases with increasing elasticity ratio of droplet to matrix phase.

The alignment of droplet under shear flow was observed by Migler (2000). The deformation of elastic droplets in a polymeric matrix under a shear flow was studied in order to find the conditions in which droplets can align in the vorticity direction. The viscosity ratio is near unity, but the elasticity ratio of the droplet to the matrix is greater than 100. Under this condition, the matrix phase was nearly Newtonian. In the limit of weak shear and small droplets (Ca < 5), the droplet alignment was found to be along the flow direction (shear direction), in contrast for a strong shear and large droplets (Ca > 5), the droplet alignment was along the vorticity direction with a broad distribution of aspect ratios.

Hayashi et al. (2000) observed the shape recovery of a deformed droplet in an immiscible polymer matrix under large step strains. They discovered that after applying a large step strain, a spherical droplet in a matrix with higher viscosity deformed to a flat ellipsoid. Then the flat ellipsoid changed into a rod-like shape, to a dumbbell and to an ellipsoid in revolution. Finally, its shape relaxed back to the sphere. The shape recovery can divide into three stages. The early stage of the shape recovery, the large reduction of surface area occurs by changing the shape from the flat ellipsoid to the rod-like without reducing droplet stretch. At the intermediate stage, the further reduction occurs slowly by reducing the droplet stretch. The capillary instability also appears at this stage but the reduction of the surface area due to this instability is small. In the last stage, the droplet recovers the spherical shape depending on the initial radius of droplet. The time needed for this process increases with the increasing initial radius of droplet and with increasing strain. They also observed the orientation angle between major axis and shear direction (flow direction) during this recovery process. They found that the orientation remained the same.

Mighri and Huneault (2001) studied the deformation and the breakup of a single droplet of a viscoelastic Boger fluid in a Newtonian matrix, sheared in a transparent Couette flow cell. At low shear rate, they found that the steady-state

deformation increased with shear rate as expected, but above a critical shear rate (Ca $\approx$ 5) the deformed drop began contracting in the flow direction and changed its orientation to the vorticity axis. With further increases in shear rate, this elongation in the vorticity direction increased until breakup finally occurred at a capiiiary number no higher than Ca $\approx$ 35. They proposed that the critical shear stress for reorientation of the droplet in the vorticity direction was probably related to the values of the first and second normal stress differences and their dependencies on shear rate.

Newtonian drops in Newtonian suspending fluid and Newtonian drops in viscoelastic suspended fluid were investigated by Ha and Leal (2001). The stability of drops following the cessation of flow in each case was determined. If the ratio between extended lengths to initial radius is high enough, the drops will break into two or more parts as known as end-pinching. However, in the Newtonian/Newtonian system, the critical degree of stretch for breakup increases with increasing capillary number. Moreover, for a Newtonian drop in a Newtonian fluid, their stability is slightly less than that of the same drops in a viscoelastic fluid.

Lerdwijitjarud *et al.* (2003) showed that in a 20% blend of a Newtonian liquid in a Newtonian matrix the steady-state capillary number is actually lower than the critical capillary number for breakup of an isolated droplet, i.e., the disturbances to the flow produced by the presence of other droplets enhance breakup of a given droplet to an extent that more than offset any increase in droplet size due to coalescence. Thus, the high steady-state capillary numbers observed in blends of viscoelastic polymers must be attributed to the role of viscoelasticity.

Recently, single viscoelastic droplets in Newtonian or viscoelastic matrices have been observed microscopically in simple shearing flows. Lerdwijitjarud *et al.* (2003) observed deformation and breakup of isolated droplets of weakly elastic fluid ($Wi_d \leq 0.02$) in a Newtonian matrix, and found that droplet clasticity produces a slight (up to around 20%) increase in Ca_c, the critical capillary number for droplet breakup. The breakup mechanism appeared to be similar to that in a Newtonian fluid; i.e., the droplet deformed increasingly in the flow direction as the shear rate was gradually

increased, until breakup occurred. Elasticity of the droplet produced a reduction in the degree of deformation at any given shear rate and a greater critical deformation at breakup, resulting in a higher Ca_c. However, at the highest Weissenberg number (Wi_d), this effect appeared to be saturating, leading to only a modest increase in Ca_c.

In 2004, Lerdwijitjarud *et al.* studied the elasticity of droplet by adding high molecular weight polybuadiene into low molecular weight polybutadiene dispersed phase and blend with polydimethylsiloxane matrix. They found that the steady state deformation of isolated droplet decreasing with increasing dispersed phase elasticity at the same imposed capillary number. They also found the relationship between critical capillary number (Ca_c) and dispersed phase Weissenberg number (Wi_d). The linear relationship holds up to a value of Wi_d equal to one and Ca_c approach to asymptotic value of 0.95 for high Wi_d. The steady state capillary number (Ca_{ss}) that calculated from average droplet diameter for 10%-dispersed phase blends is less than the Ca_c for isolated droplets for the same blends.

Cherdhirankorn *et al.* (2004) measured the dynamics of deformation of an elastic droplet in an elastic matrix. Both two polymers have the same viscosity but differing degree of elasticity. The different elasticities produce qualitative differences in the droplet deformation occur before the droplet attains its steady state shape. For the system with higher elasticity, the deformation oscillates several times before reaching its steady state shape, but for the lower elasticity system, the droplet deforms in shear direction first and continuously contacts in the flow direction until reaching its steady state shape. The capillary number can be varied at fixed elasticity and shear rate by increasing the droplet size. The steady state shape of both systems deform increasingly along the vorticitiy direction.

Wannaborworn and Mackley (2002) used optical shearing apparatus and modified rheometer to observe the deformation and breakup of immiscible drops with a viscosity ratio around unity under oscillatory shear. For moderate strain, the drop deformation oscillates between maximum and non-zero minimum deformation

parameter. For large strain, the drops breakup occur only by one mechanism. It is called end pinching.

II. EXPERIMENTS

A. Materials

The materials used in this study were polydimethylsiloxanes, PDMS, of different viscosity values: 60,000 centiStoke (Viscasil 60M), 30,000 centiStoke (Viscasil 30M) and 10,000 centiStoke (Viscasil 10M) (Donated by General Electric International Operations Company Inc.) as the matrix phases and a polybutadiene, PBd (Ricon 150, donated by Chemical Innovation) as the dispersed phase. The properties of the blend components are listed in Table I. High-molecular-weight polybutadiene (M_w ~841,000, M_w/M_n ~1.20 purchased from Fluka Chemical Corp.) was used as a high molecular weight polymer component additive for the Ricon 150 to make a "Boger" fluid [Binnington (1977)] with significantly higher elasticity but a slight shear thinning behavior. The polymer blend systems are listed in Table II and Table III.

B. Sample Preparation

PDMS's were used as received. Because of volatile components in PBd as received, it had to be vacuum dried at 50 °C until all volatile components were driven off and the weight loss discontinued. The disperse phase in System 2 was prepared by completely dissolving a ten percent of high molecular weight PBd into chloromethane. The solution was mixed with low molecular weight PBd at room temperature so as to get a "Boger" fluid (Boger and Binnington, 1977). The mixture was left for five days to obtain a homogenous solution. The chloromethane and other volatile components were removed by vacuum dried at 50 °C.

C. Rheological Characterization

The storage modulus (G') and loss modulus (G") of each blend component were measured by a cone and plate rheometer (Rheometrics Scientific, model ARES, NJ), with 25-mm plate diameter with cone angle of 0.04 rad. Because of the difference in temperature dependence of the viscosities of PBd and PDMS, the equiviscosity condition, the desired viscosity ratio and G" ratio can be obtained by adjusting the operating temperature. Each polymer was molded into a cone and plate fixture with a gap of 0.051 mm. From the rheological properties of pure polymers at various temperatures, the desired pairs of polymers and operating temperatures were selected for further study. The rheological properties are shown in Fig. 1. In this study, we investigated the system 1 at G" ratios equal to 0.16, 1 and 3 and the corresponding G' ratios are 0.16, 1.0 and 3.0 at the temperatures of 67, 33 and 20 °C, respectively. Since G" >> G' at all frequencies and all temperatures investigated, the blend system 1 can be considered a pure viscous fluid containing nearly zero viscosity.

D. Observation of an Isolated Droplet in Shearing Flow

1. Shearing Apparatus

To observe the droplet behaviors in an oscillatory shear flow, we used a flow cell (Linkam CSS 450, Linkam Scientific Instruments Ltd., UK) consisting of two transparent quartz parallel disks mounted on an optical microscope (Leica DMRPX, Leica Imaging Systems LTd., Cambridge, England), and connected to a CCD camera (Cohu 4910, Cohu Inc., CA). In addition, the images were analyzed on a computer using the Scion image software (U.S. National Institutes of Health, www.scioncorp.com). In case of isolated droplets, the PDMS matrix phase was first loaded into the flow cell. The PBd disperse phase, an isolated single droplet, was inserted into the matrix phase by using a microsyringe. To prevent the droplet from migrating away from the wall, the droplet at the center of the gap was chosen for the study.

2. Droplet Shape Relaxation Time

Here, we determined the interfacial tensions of various systems studied. The samples were loaded into the flow cell, and the temperature was adjusted to obtain a desired G" ratio. We selected the droplet with the initial size of around 200 ($\pm$10%) μm. The step strains that we imposed to the sample were 0.5-20% with the shear rates of 1, 2 and 3 rad/s. The deformation of the isolated droplet shape after a step strain was recorded and the deformation parameters (Def (Eq. 2)) were determined to obtain a time series of the retracting droplet deformation Def* vs. time, which has been known to decay exponentially as [Lucinia et al. (1997)]:

$$Def = Def_o \exp\left(-\frac{t}{\tau}\right) \qquad (3)$$

The characteristic relaxation time for a single isolated droplet (τ) can be derived from semi-logarithmic plots of droplet deformation versus relaxation time. The slope of the straight line fitted to the data in the linear relaxation regime [Luciani et al. (1997), Mo et al. (2000), Xing et al. (2000)]. By equating this characteristic relaxation time to that predicted by the Palierne model (Eq.3) [Palierne (1990) and Graebling et al. (1993)], the interfacial tension was then calculated from the following relation:

$$\tau = \frac{(3 + 2\eta_r)(16 + 19\eta_r)r_o\eta_{m,o}}{40(1 + \eta_r)\Gamma} \qquad (4)$$

where $\eta_r = \eta_d/\eta_m$ is the ratio between the dispersed phase viscosity and the matrix phase viscosity, Γ is the interfacial tension and r_o is the radius of the spherical drop. To obtain images of the relaxation droplet after a step strain, the desired strain was imposed onto a selected droplet in the field of view of the microscope. The droplet was then allowed to relax. Two hundred to three hundred images were then recorded (ten to twenty frames per second) while the droplet relaxed its shape to its original sphere shape.

Using the optical microscope, the droplet images were captured only from the top view, this view cannot measure the true lengths of the principle axes. However, the lengths of these axes can be determined by using the affine angle of rotation of the

droplet in plane containing the flow and shear-gradient directions (Larson 1988) together with the condition of volume preservation, D_o^3 = abc (Almusallam *et al.* (2000)). Although the lengths of the principle axes can be appropriated by using the method mentioned above, we use the apparent lengths of the observable axes, to describe the behavior of each droplet. We can define a modified deformation parameter Def* as:

$$\text{Def}* \equiv \frac{a*-c}{a*+c} \tag{5}$$

where a* and c are major and minor axis of droplet images obtain from top view.

3. Oscillatory Deformation

This experiment is similar to the relaxation experiment, where a sample was loaded and the operating temperature and the size of the droplet were chosen. Now, the shearing mode was oscillatory. The Linkham device, which has one stationary and one moving plate, inevitably caused the droplet move back and forth. Before we started each experiment the drop was allowed for relax until it retained a spherical shape. Appropriate strain and frequency were then chosen.

The characteristic time scale ratio (τ_r), equal to the characteristic relaxation time scale (τ_{rel}) over the oscillatory time (τ_{osc} = 1/f), is used to describe the ability of drop to relax under an oscillatory shear flow at various frequencies. For the system 1, at the viscosity ratio equal to one, we investigated at τ_r equal to 0.04, 0.2 and 1 corresponding to oscillating frequencies of 0.02, 0.1, and 0.5 Hz, respectively.

For a given frequency, we increased the strain until we could no longer capture the complete images during a droplet deformation cycle. For a droplet deformation, six hundred and seven hundred images were recorded; for each period of deformation the numbers of captured images were equal to or above 32 in order to track the deformation time series in details. The droplet deformation, major and minor axes were measured as function of time, frequency, strain, G" ratio, and G' ratio.

III. RESULTS AND DISCUSSION

A. Rheological Characterization

The rheological property of the blend components was obtained from the fluid rheometer (ARES, NJ). Figures 1.1 and 1.2 show the storage modulus (G') and the loss modulus (G"), respectively. The data indicate that the two polymers behave according to Maxwell's fluid because the slope of G' is approximately equal to two and the slope of G" is approximately equal to one. G' and G" vary with the temperature; the values become smaller as temperature is higher. Polydimethylsiloxane has a higher temperature-dependent viscosity than that of polybutadiene, allowing us to obtain the desired G' and G" values by adjusting operating temperature. Alternatively, we can vary the G' and G" ratios by using different molecular weights without changing the temperature. However, this later method is more time consuming and difficult to obtain desired ratios in practice. The values of the G' and G" ratios are shown in Figure 1.3.

In our experimental, the working fluid is highly viscous so G" ratio is relevant while G' ratio is not. In our experiment, G" ratio is equal to 0.16, 1 and 3 at 67°C, 33°C and 20°C, for 0.02% high Mw PBd sol^n and 0.05% high Mw PBd sol^n, G"ratio isequal to 1 at 27 °C and 25°C respectively, at all frequencies examined.

B. Relaxation Experiment

The relaxation time scale of each blend studied was obtained from a step strain experiment using various shear rates and drop sizes. Appropriate strain rate and drop size were then chosen so that the relaxation time obtained is independent of the strain rate used or drop size chosen The values of interfacial tension values obtained are 3.5×10^{-3} N/m, 2.9×10^{-3} N/m and 2.67×10^{-3} N/m with the characteristic times equal to 5.1 sec., 1.9 sec and 0.585 sec, for G"$_r$ equal to 0.16, 1 and 3. For 0.02% high Mw PBd sol^n and 0.05% high Mw PBd sol^n, the interfacial tension values are equal to 3.0×10^{-3} N/m and 3.02×10^{-3} N/m with the characteristic times equal to 2.02 sec.and 2.3 sec, respectively.

C. Oscillatory Shear Experiment

In this study, since there are many parameters involved, we grouped them into dimensionless pi groups; they are Capillary Number (Ca_m), Reynolds number (R_e), and the time scale ratio (τ_r) and Weissenberg number. Ca_m and R_e are defined as:

$$Ca = \frac{G_m{''}(\omega)\gamma d}{\Gamma} \qquad (6)$$

$$Re = \frac{\rho_d \omega^2 d^2}{G_d{''}(\omega)} \qquad (7)$$

where γ is the strain that we imposed onto the blends, d is the diameter of droplet, $G_m{''}(\omega)$ is the loss modulus of the matrix phase, $G_d{''}(\omega)$ is the loss modulus of the disperse phase, ρ_d is the density of the disperse phase, and Γ is the interfacial tension between two polymers. The time scale ratio is defined as:

$$\tau_r = \tau_{rel}/\tau_{osc} \qquad (8)$$

where τ_{rel} is the relaxation time scale obtained from the relazation experiment, τ_{osc} is the period of oscillation, $\tau_{osc} = 1/f$ where f is the oscillation frequency imposed.

The Weissenberg number, which is a dimensionless number used in the study of viscoelastic flows, is defined as the ratio of the first normal stress difference to twice the shear stress at the imposed shear rate.

$$Wi_d = 2G_d'(\omega)/G_m{''}(\omega)\gamma \qquad (9)$$

The values of the Weissenberg number for blend systems are shown in table2, 3 and 4 : system A1 ($G_r{''} = 0.16$), $Wi_d = 0.0006$-0.006; system A2 ($G_r{''} = 1$, $\tau_r = 0.2$), $Wi_d = 0.0034$-0.034; system A2 ($G_r{''} = 1$, $\tau_r = 0.57$), $Wi_d = 0.0045$-0.045; system A2 ($G_r{''} = 1$, $\tau_r = 1$), $Wi_d = 0.0057$-0.057; system A3 ($G_r{''} = 3.0$), $Wi_d = 0.0092$-0.092; system B1 (0.02%high M_w PBd sol$_{-}^n$, $G_r{''} = 1$), $Wi_d = 0.006$-0.068; system B2 (0.05%high M_w PBd sol$_{-}^n$, $G_r{''} = 1$), $Wi_d = 0.018$-0.186.

In our study, we divided our work into 3 parts: effect of viscosity ratio, effect of time scale ratio, and effect of elasticity ratio.

Figure 2 shows experimental photographs of a droplet under oscillatory deformation, $G''_r = 1$, $Ca_m = 0.8$, $Re_{osc} = 2.0186*10^{-8}$, $\tau_r = 0.2$. The drop size was 200 μm. The droplet can be seen to stretch along the flow direction, to retract to its original value, to stretch again, and finally to retract back when the cycle is complete, or when the observation time over the oscillatory time scale ratio is one. We may note that droplet deformation in oscillatory shear as seen is more complicated than that in steady shear due to the combination of the droplet rotation and the periodic change in shear direction.

Figure 3 shows the time series of the deformation amplitudes, a*, c, and Def* vs. time for the droplet of Figure 2. We can clearly see that there is an initial transient deformation, lasting about 8 seconds, prior to the final steady state oscillatory deformation taking place. In the final steady state oscillatory shear deformation, we can define the deformation amplitudes as the one half of the differences between the maximum and the minimum vales of the corresponding deformation parameters: a*, c, and Def*, respectively.

Figures 4a, 4b, and 4c show the deformation amplitudes δa*, δc, and δDef* vs. Ca_m for the three blend systems studied: $G''_r = 0.16$, 1.0 and 3.0. In these experiments, the oscillatory frequency was chosen to be 0.35 Hz, 0.1 Hz, and 0.04 Hz, respectively so that the corresponding time scale ratios are all equal to 0.2. We can see that, for a given Ca_m, Def* is greater for a droplet with a smaller viscosity ratio. This implies that droplet viscosity resists droplet oscillatory deformation, a similar finding to that of the steady state shear flow. From Figure 4c, we may note that the relation between Def* and Ca_m is linear when the viscosity ratio is 0.16 or 1.0. This may stems from the fact that for these two blends Ca_m was restricted to be small and below 1.2. On the other hand, for the blend of viscosity ratio equal to 3.0, the relation between Def* and Ca_m has two regimes: a linear relation when Ca_m is below 2.2; a nonlinear relation when Ca_m is greater than 2.2. We can identify that the critical Ca_m for the nonlinear oscillatory

deformation to be about 2.2. We also note that the deformation frequency measured for these blends at various Ca_m still remains nearly the same as the excitation frequency, f_{osc}.

Figure 5a, 5b and 5c show the deformation amplitudes δa^*, δc, and δDef^* vs. Ca_m for the four blend systems studied: $\tau_r = 0.2$, 0.57, and 1. The corresponding G''_r is all equal to one. We can see that, for a given Ca_m, Def^* is greater for a droplet with a smaller time scale ratio τ_r. Smaller time scale ratio means that droplet relaxes very fast relative to the deformation time scale and the droplet tends to be close to the equilibrium deformation at any instant. On the other hands, when the time scale ratio is much larger than one droplet cannot adjust itself fast enough to be in the equilibrium deformed state at a particular instant, so that the apparent deformation observed is far from equilibrium. In the limit of τ_r approaches zero we would expect the Def^* vs. Ca_m to rise towards its asymptotic limit. In the limit of τ_r becomes very large, we would expect that Def^* would become independent of Ca_m and a rigid body translation would be observed.

Figures 6a, 6b and 6c show the amplitude of deformation parameter δa^*, δc, and δDef^* vs. Ca_m for the effect of elasticity studied systems: No elasticity, 0.02% high Mw PBd sol^n and 0.05% high Mw PBd sol^n. The time scale ratio and G''_r were fixed at 0.2 and 1. The oscillatory frequency was selected to be 0.1 Hz for no elasticity system, 0.099 Hz for 0.02% high Mw PBd sol^n and 0.087 Hz for 0.05% high Mw PBd sol^n. We can observe that, for a small given Ca_m, the amplitude of deformation parameters at different elasticity are almost the same, but when the Ca_m is higher, the non elastic drop deforms greater than elastic drop. It can be implied that the elastic drop resists droplet oscillatory deformation.

Figures 7 and 8 show experimental photographs of a drop breakup under oscillatory deformation at minimum critical capillary number, for frequency equal to 0.05 Hz and 0.1 Hz. The corresponding time scale ratios are 0.029 and 0.0585. The original drop size was 150 μm, $G''_r = 0.16$. At frequency equal to 0.05 Hz, drop can be seen to stretch along the flow direction. As the amplitude of oscillation was increased the drop progressively deformed and at the critical condition, the usual dumbbell shape breakup patterned was observed. The drop broke into two parts. For frequency equal to

0.1 Hz, the breakup mechanism is similar to that of 0.05 Hz, but the different is the number of small drops after breaking; now it has three daughter drops. The higher frequency yields smaller drop sizes after breaking relative to those of the lower frequency.

Figure 9 shows the minimum critical capillary number vs. time scale ratio, at T = 67 °C, G''_r = 0.16. Droplet size was 150 μm. We can observe that at higher time scale ratio (high frequency), the higher capillary number is required to obtain the drop breakup.

IV. CONCLUSIONS

Experimental of droplet deformation in oscillatory shear have been presented in this work. Three effects of drop deformation have been studied: the effect of viscosity ratio; the effect of time scale ratio; the effect of elasticity.

For oscillatory deformation of droplet in different viscosity ratios and fixed time scale ratio, the capillary of the high viscosity ratio system is higher than the small viscosity ratio system at the same amplitude of deformation. It can be implied that the droplet with a higher viscosity ratio has higher ability to resist the oscillatory deformation than the droplet with a low viscosity ratio.

For the effect of different time scale ratio and with G''_r equal to unity, we found that the amplitude of deformation is higher with the small time scale ratio. It can be concluded that when the time scale ratio is high the drop cannot itself fast enough so it behaves like a solid where small deformation would be observed. On the other hand, for low time scale ratio, the time is long enough to allow the drop to behave like a liquid. Droplet can be deformed easier than droplet with a higher time scale ratio.

For the effect of elasticity, the drop which does not has elasticity deformed more than the elastic drop. The elasticity of droplet prevents the oscillatory deformation.

The breakup of Newtonian drops in an oscillatory flow seems to be similar to the steady shear case. The breakup mechanism occurred through the dumbbell pattern.

The higher oscillatory frequency induces more daughter drops than low frequency. The minimum critical capillary number of the high frequency is higher than that of the low frequency.

ACKNOWLEDGEMENTS

References

Bertalan, Gy., Marosi, Gy., Anna, P., Ravadits, I., Csontos, I., and Tóth, A. "Role of interface modification in filled and flame-retarded polymer systems," Solid State Ionics, 141-142, 211-215 (2001).

Bentley, B.J., and Leal, L.G. "An experimental investigation of drop deformation and breakup in steady, two-dimensional linear flows," J Fluid Mech, 167, 241-283 (1986).

Boger, D.V., and Binnington, R.J. "Separation of elastic and shear thinning effects in the capillary rheometer," Trans. Soc Rheol, 21, 515-534 (1977).

Cherdhirankorn, T., Lerdwijitjarud, W., Sirivat, A., and Larson, R. G. "Dynamics of vorticity alignment and breakup of isolated viscoelastic droplets in an immiscible viscoelastic matrix" Rheol. Acta, 43:246-256 (2004).

Elmendorp, J.J. "A study on polymer blending microrheology," Polymer Engineering Science, 26, 418-426 (1986).

Elmendorp, J.J., and Maalcke, R.J. "A study on polymer blending microrheology: part1," Polymer Engineering Science, 25, 1041-1047 (1985).

Grace, H.P. "Dispersion phenomena in high viscosity immiscible fluid systems and application of static mixers as dispersion devices in such systems," Chemical Engineering Communication, 14, 225-227 (1982).

Guido, S., and Villone, M. "Three-dimensional shape of a drop under simple shear flow," J Rheol, 42, 395-415 (1998).

Ha and Leal "An experimental study of drop deformation and breakup in extensional flow at high capillary number," Physics of fluids, 13, 1568-1576 (2001).

Hayshi, R., Takahashi, M., Kajihara, T., and Yamane, H., "Dynamic interfacial properties of polymer blends under large step strains; shape recovery of a single droplet," Polymer, 42, 757-764 (2000).

Lerdwijitjarud, W., Sirivat, A., and Larson, R.G. "Influence of elasticity on dispersed-phase droplet size in immiscible polymer blends in simple shearing flow," Polymer Engineering Science, 42, 798-809 (2002).

Lerdwijitjarud, W., Larson, R.G., Sirivat, A., and Solomon, M.J. "Influence of weak elasticity of dispersed phase on droplet behavior in sheared polybutadiene/ Poly(dimethylsiloxane) blends," J Rheol, 47, 37-57 (2003).

Lerdwijitjarud, W., Sirivat, A., and Larson, R.G. "Influence of dispersed-phase elasticity on steady state deformation and breakup of droplets in simple shearing flow of immiscible polymer blends," J. Rheol, 48, 843-862 (2004).

Mighri, F., Carreau, P.J., and Ajji, A. "Influence of elastic properties on drop deformation and in shear flow," J Rheol, 42, 1477-1490 (1998).

Mighri F., and Huneault M.A. "Dispersion visualization of model fluids in a transparent Couette flow cell," J Rheol, 45, 783-797 (2001).

Migler, K.B. "Droplet vorticity alignment on model polymer blends," J Rheol, 44, 277-290 (2000).

Mo, H., Zhou, C., and Yu, W. "A new method to determine interfacial tension from the retraction of ellipsoidal drops," J. Non Newtoniam Fluid Mech. 91, 221-232 (2000).

Palierne, J.F. "Linear rheology of viscous properties of emulsions with interfacial tension," Rheol. Acta, 29, 204-214 (1990).

Rumscheidt, F.D., and Mason, S.G. "Particle Motions in Sheared Suspensions. XII. Deformation and burst of fluid drops in shear and hyperbolic flow," J Coll Sci, 16, 238-261 (1961).

Taylor G.I. "The viscosity of a fluid containing small drops of another fluid," Proc. R. Soc A, 138, 41-48 (1932).

Taylor G.I. "The formation of emulsions in definable fields of flow," Proc R Soc A, 146, 501-523 (1934).

Wannaborworn S., Mackley M. R., and Renardy Y. "Experimental observation and matching numerical simulation for the deformation and breakup of immiscible drops in oscillatory shear," J Rheol, 46(5), 1279-1293 (2002).

Table I Polymers used

Polymers	Suppiers	M_n	Specific gravity
Low M_w PBd	General Electric International Operations Company Inc.	3,900	0.89
High M_w PBd	Aldrich Chemical Company, Inc.	702,000	1.2
PDMS	Chemical Innovation	91,700	0.976

Table II Effect of viscosity ratio

Blend system	Blend components	T (°C)	Γ (mN/m)	G''_r	Wi_d	f (Hz)	τ_{rel} (sec)	τ_{osc} (sec)	Time scale ratio (τ_r)
A1	PBd/PDMS	67	3.5	0.16	0.0006-0.006	0.35	0.585	2.857	0.2
A2	PBd/PDMS	33	2.9	1.0	0.0034-0.034	0.3	1.9	3.33	0.2
A3	PBd/PDMS	20	2.67	3.0	0.0092-0.092	0.04	5.1	25	0.2

Table III Effect of time scale ratio ($\tau_r = \tau_{rel}/\tau_{osc}$)

Blend system	T (°C)	Γ (mN/m)	G''_r	Wi_d	f (Hz)	τ_{rel} (sec)	τ_{osc} (sec)	Time scale ratio (τ_r)
A2	33	2.9	1.0	0.0034-0.034	0.1	1.9	10	0.2
A2	33	2.9	1.0	0.0045-0.045	0.3	1.9	3.33	0.57
A2	33	2.9	1.0	0.0057-0.057	0.52	1.9	1.9	1.0

Table IV Effect of elasticity ratio

Blend system	Blend Components	T (°C)	Γ (mN/m)	G''_r	Wi_d	f (Hz)	τ_{rel} (sec)	τ_{osc} (sec)	Time scale ratio (τ_r)
A2	PBd /PDMS	33	2.9	1.0	0.0034-0.034	0.1	1.9	10	0.2
B1	0.02% High PBd Sol[n] /PDMS	27	3.0	1.0	0.006-0.068	0.099	2.02	10.1	0.2
B2	0.05% High PBd Sol[n] /PDMS	25	3.02	1.0	0.018-0.186	0.087	2.30	11.5	0.2
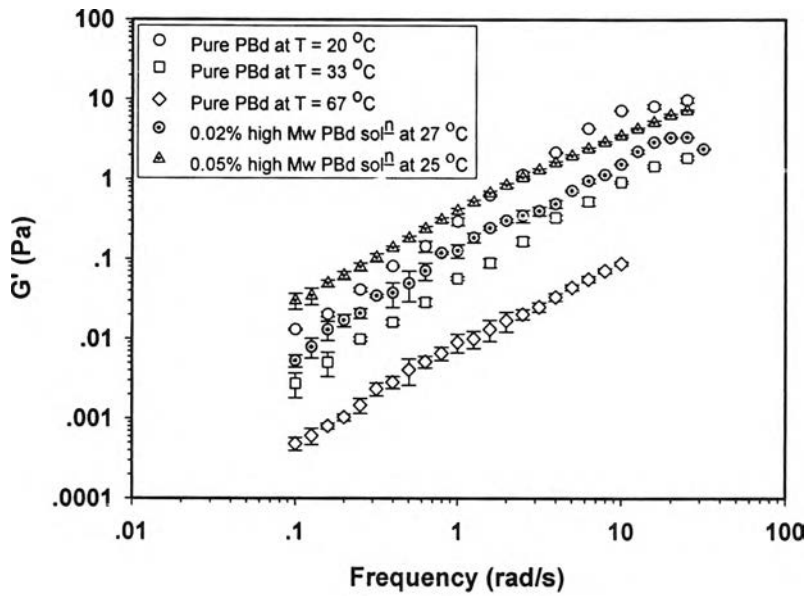
(a)
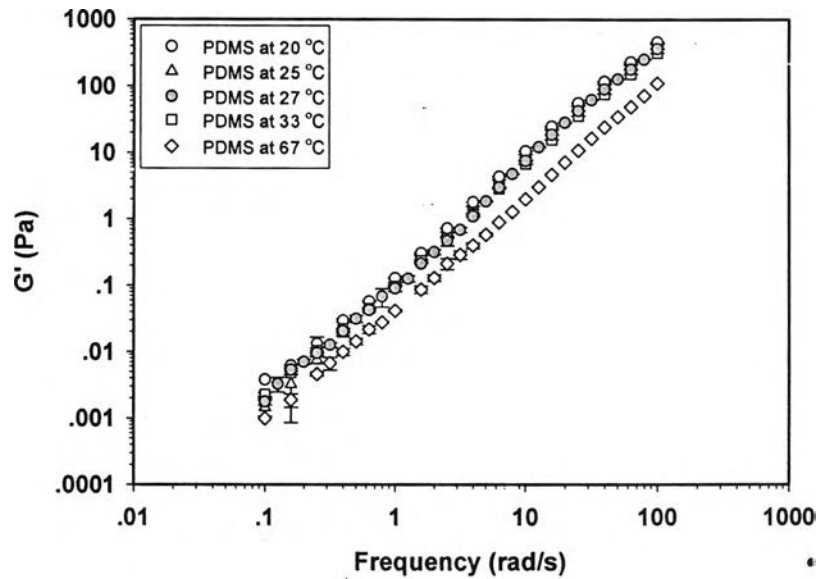
(b)

Figure 1.1 G' vs. frequency at different temperatures:

(a) dispersed phases (pure PBd, 0.02% high M_w PBd sol[n] and 0.05% high M_w PBd sol[n]) using strain = 80% at frequency 0.1-1 rad/s, and strain = 20 % at frequency 1-100 rad/s; (b) matrix phases (PDMS 30M) using strain = 80% at frequency 0.1-1 rad/s, and strain = 20 % at frequency 1-100 rad/s.
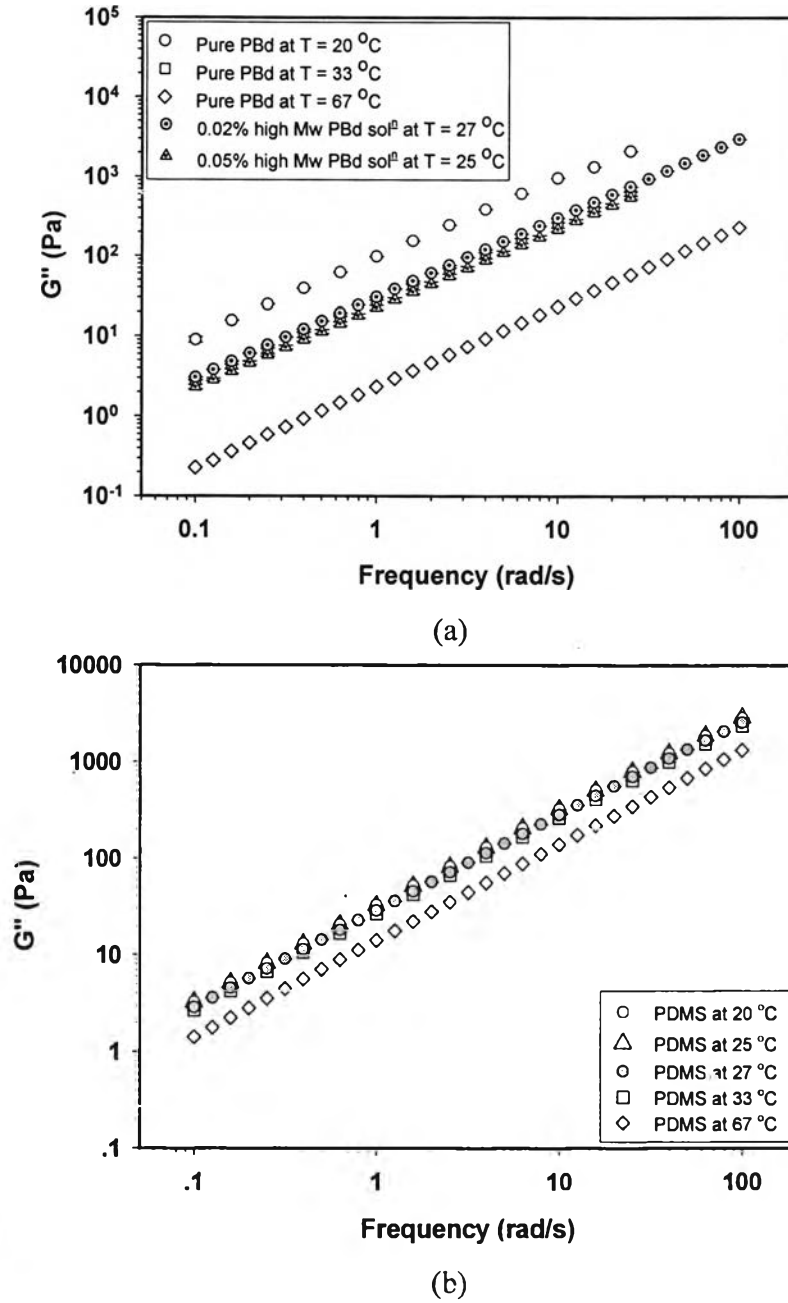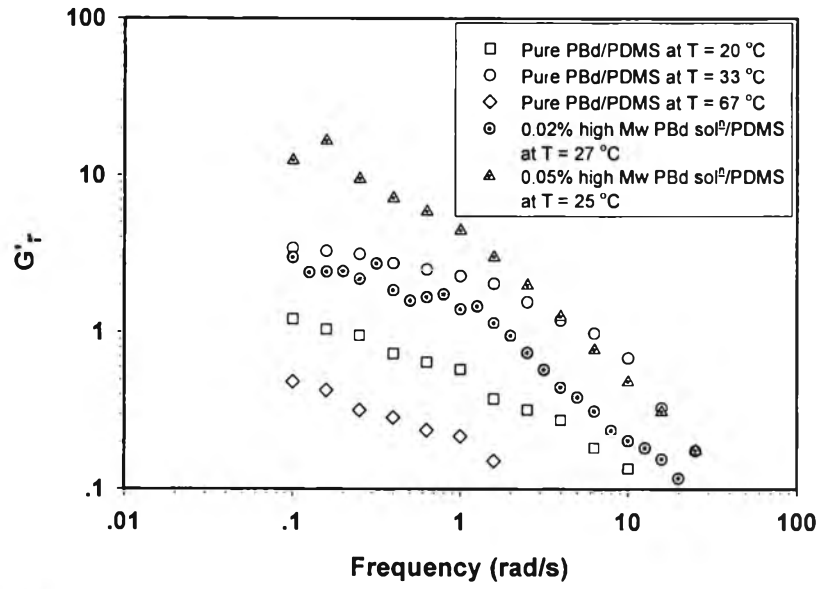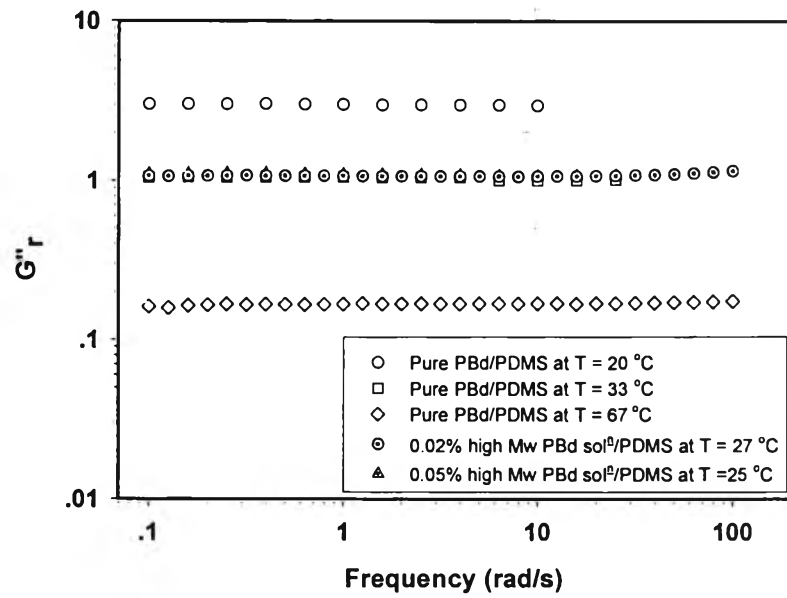
Figure 1.2 G" vs. frequency at different temperatures:

(a) dispersed phases (pure PBd, 0.02% high M_w PBd sol[n] and 0.05% high M_w PBd sol[n]) using strain = 80% at frequency 0.1-1 rad/s and strain = 20 % at frequency 1-100 rad/s ;

(b) matrix phases (PDMS 30M) using strain = 80% at frequency 0.1-1 rad/s, and strain = 20 % at frequency 1-100 rad/s.

Figure 1.3 (a) G'_r at different temperatures, (b) G''_r at different temperatures.

Time (sec)	74.58	75.08	75.59	76.09	76.59	77.09	77.58	78.09	78.58	79.09	79.58
Time/τ_{osc}	0	0.05	0.10	0.151	0.201	0.251	0.301	0.35	0.401	0.45	0.501

Time (sec)	80.08	80.58	81.08	81.58	82.09	82.59	83.09	83.58	84.08	84.58
Time/τ_{osc}	0.55	0.6	0.65	0.701	0.75	0.801	0.851	0.901	0.95	1.0
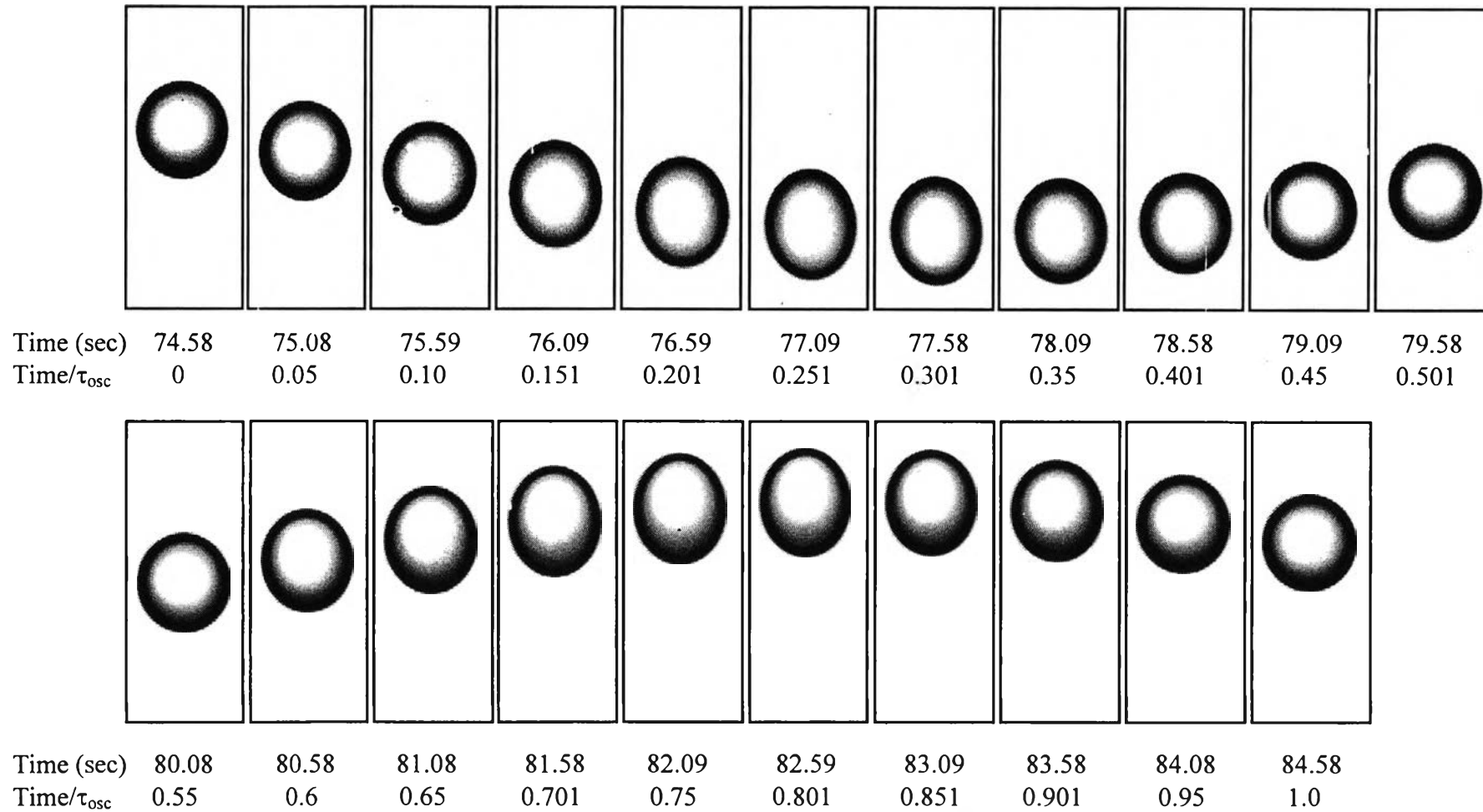
Figure 2 Droplet deformation under shear at strain = 70 %, frequency = 0.1 Hz, $G''_r = 1$, $\tau_r = 1$, T = 33 °C, $d_o \sim 200$ μm and gap 2,200 μm, at magnification 40X at various times in one cycle.
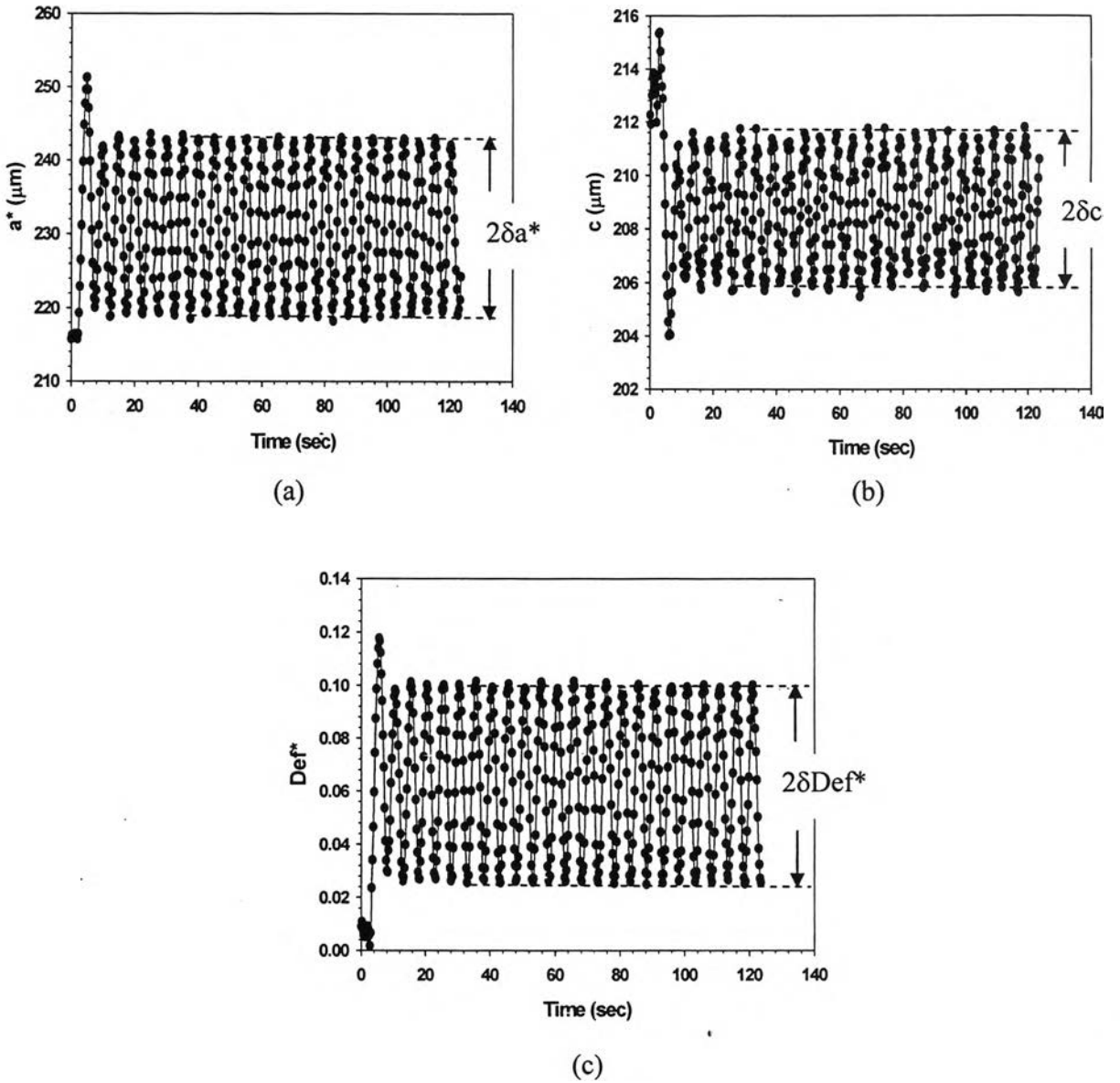
Figure 3 Deformation parameters vs. time at strain 70%, frequency 0.1 Hz, $\tau_r = 0.2$, $G''_r = 1$, $d_o = 200$ μm, gap $= 2200$ μm: a) a* vs. time; b) c vs. time; c) Def* vs. time.
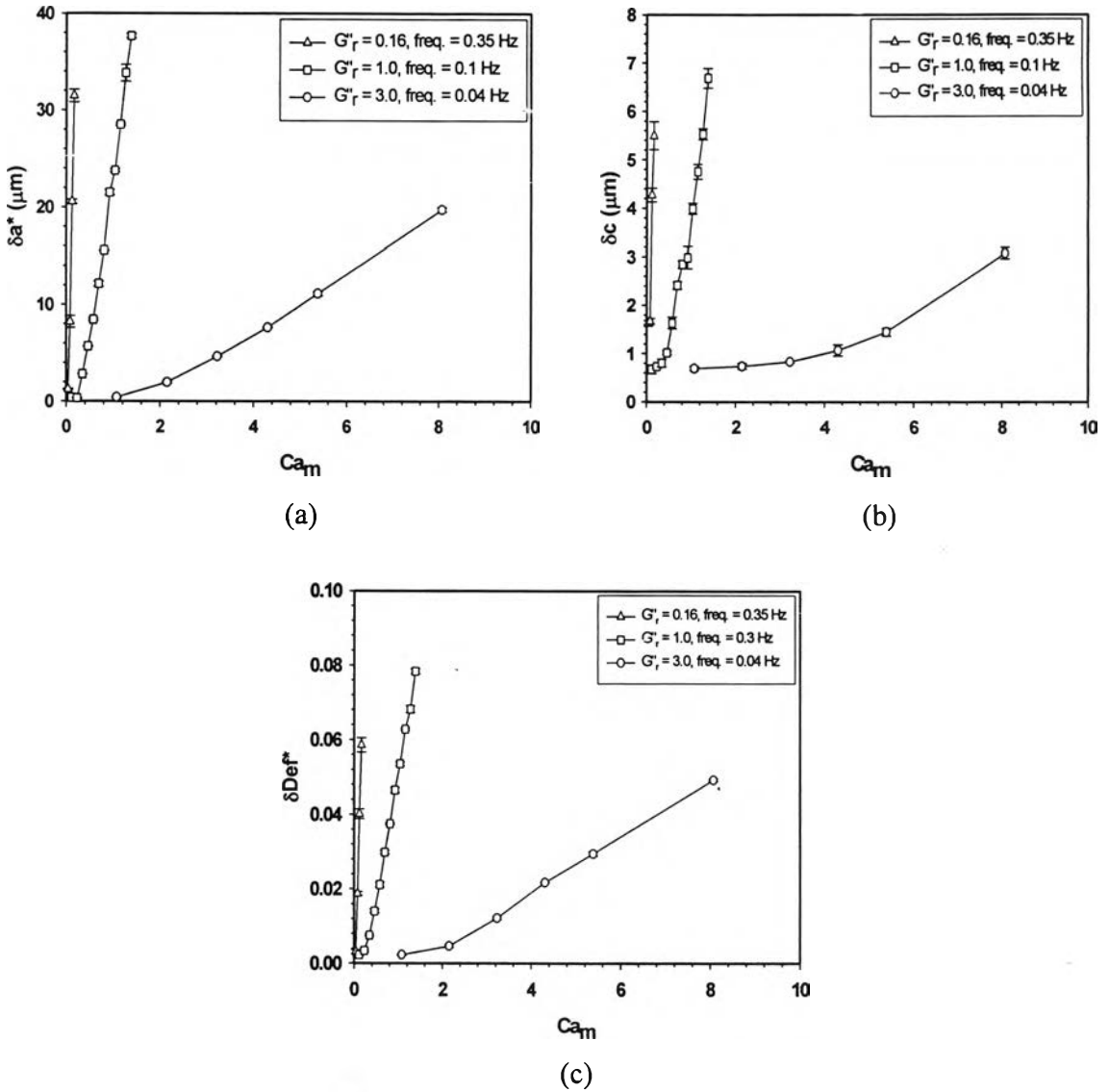
Figure 4 Amplitude of deformation parameters vs. Ca_m at $\tau_r = 0.2$, $d_o \sim 200$ μm, gap = 2,200 μm : T = 67 °C, $G''_r = 0.16$, $G'_r = 0.12$, $Re_{osc} = 7.36*10^{-6}$; T = 33 °C, $G''_r = 1.0$, $G'_r = 1.0$, $Re_{osc} = 6.081*10^{-8}$; T = 20 °C, $G''_r = 3.0$, $G'_r = 3.0$, $Re_{osc} = 2.65*10^{-10}$: distance of drop from the center of plate ~ 6.8 mm.: a) δa^* vs. Ca_m; b) δc vs. Ca_m; c) δDef^* vs. Ca_m.
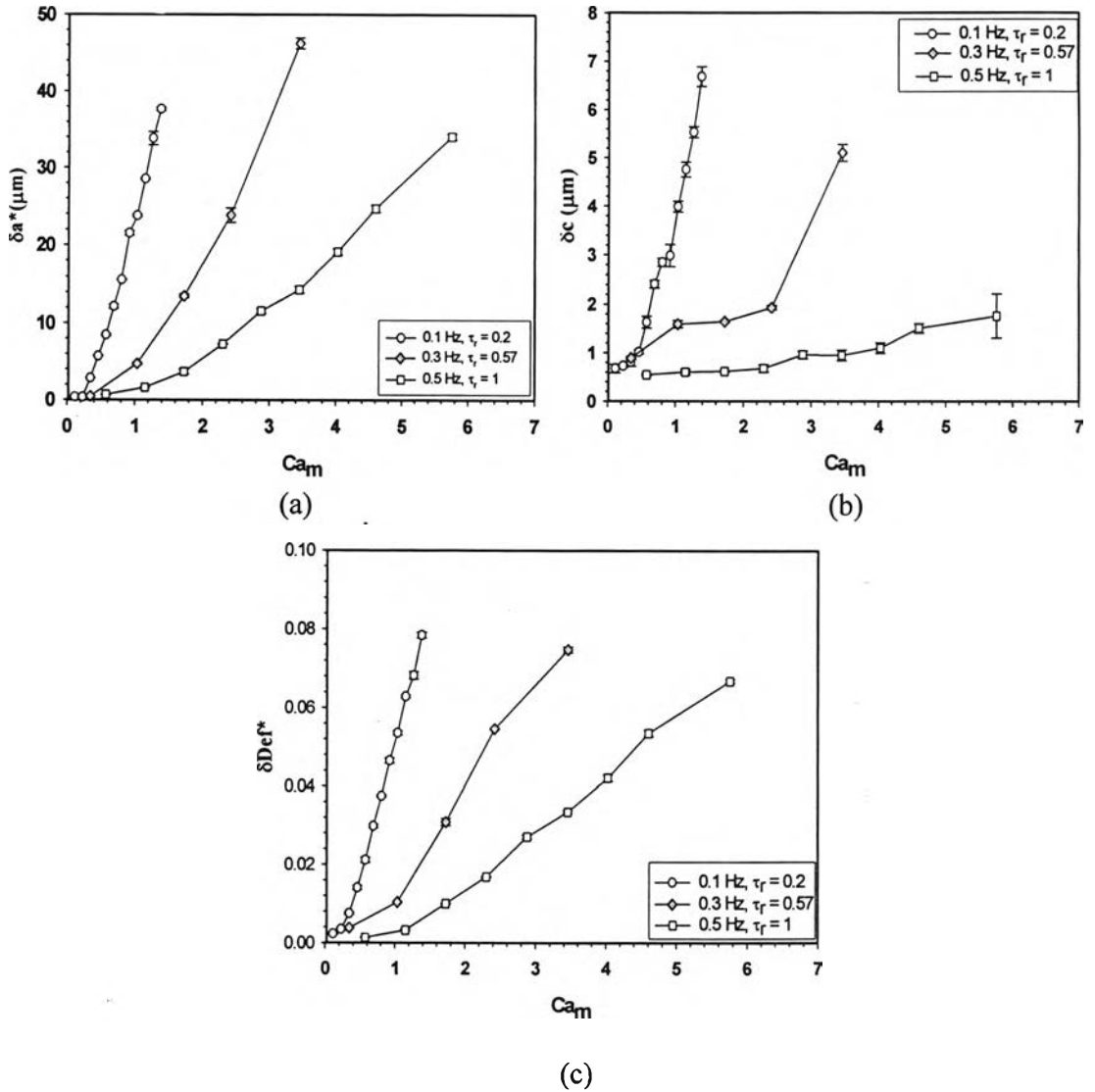
Figure 5 Amplitudes of deformation parameters vs. Ca_m at T = 33 °C, d_o = 200 μm, gap = 2,200 μm: frequency = 0.1 Hz, G''_r = 1, Re_{osc} = 2.0186*10^{-8}; frequency = 0.3 Hz, G''_r = 1, Re_{osc} = 6.081*10^{-8}; frequency = 0.5 Hz, G''_r = 1, Re_{osc} = 1.015*10^{-7}: distance of drop from the center of plate $\sim$ 6.8 mm : a) δa^* vs. Ca_m; b) δc vs. Ca_m; c) δDef^* vs. Ca_m.
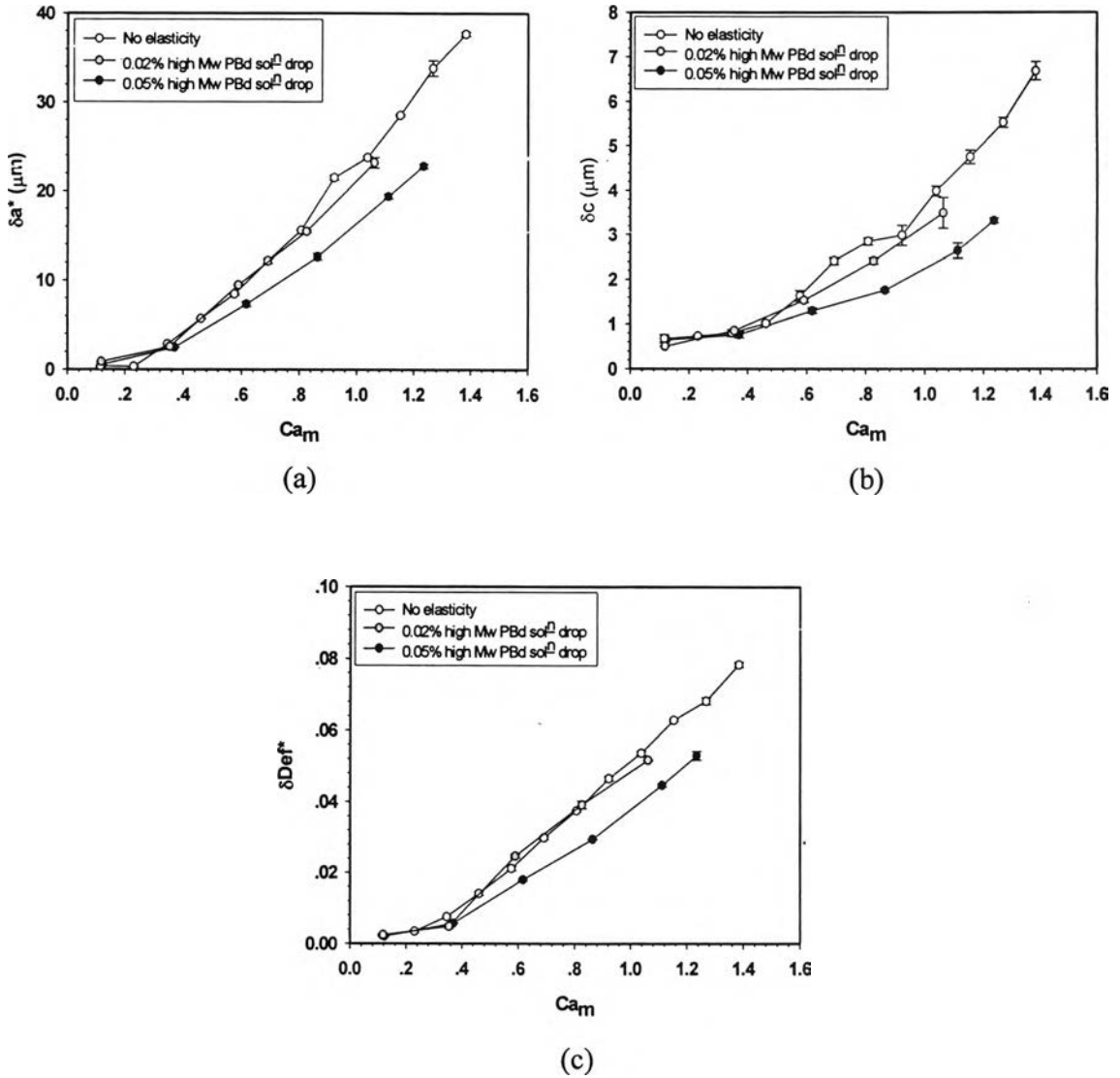
Figure 6 Amplitudes of deformation parameters vs. Ca_m at $G''_r = 1$, $\tau_r = 0.2$, $d_o \sim 200$ μm, gap = 2200 μm: of pure PBd/PDMS, T = 33 °C, freq. = 0.1 Hz, $Re_{osc} = 2.0186*10^{-8}$; 0.02 % high Mw PBd sol^n/PDMS, T = 27 °C, freq. = 0.099 Hz, $Re_{osc} = 2.3745*10^{-8}$ and 0.05% high Mw PBd sol^n/PDMS, 25°C, freq. = 0.1 Hz, $Re_{osc} = 2.7658*10^{-8}$: a) $\delta a*$ vs. Ca_m; b) δc vs. Ca_m; c) $\delta Def*$ vs. Ca_m.
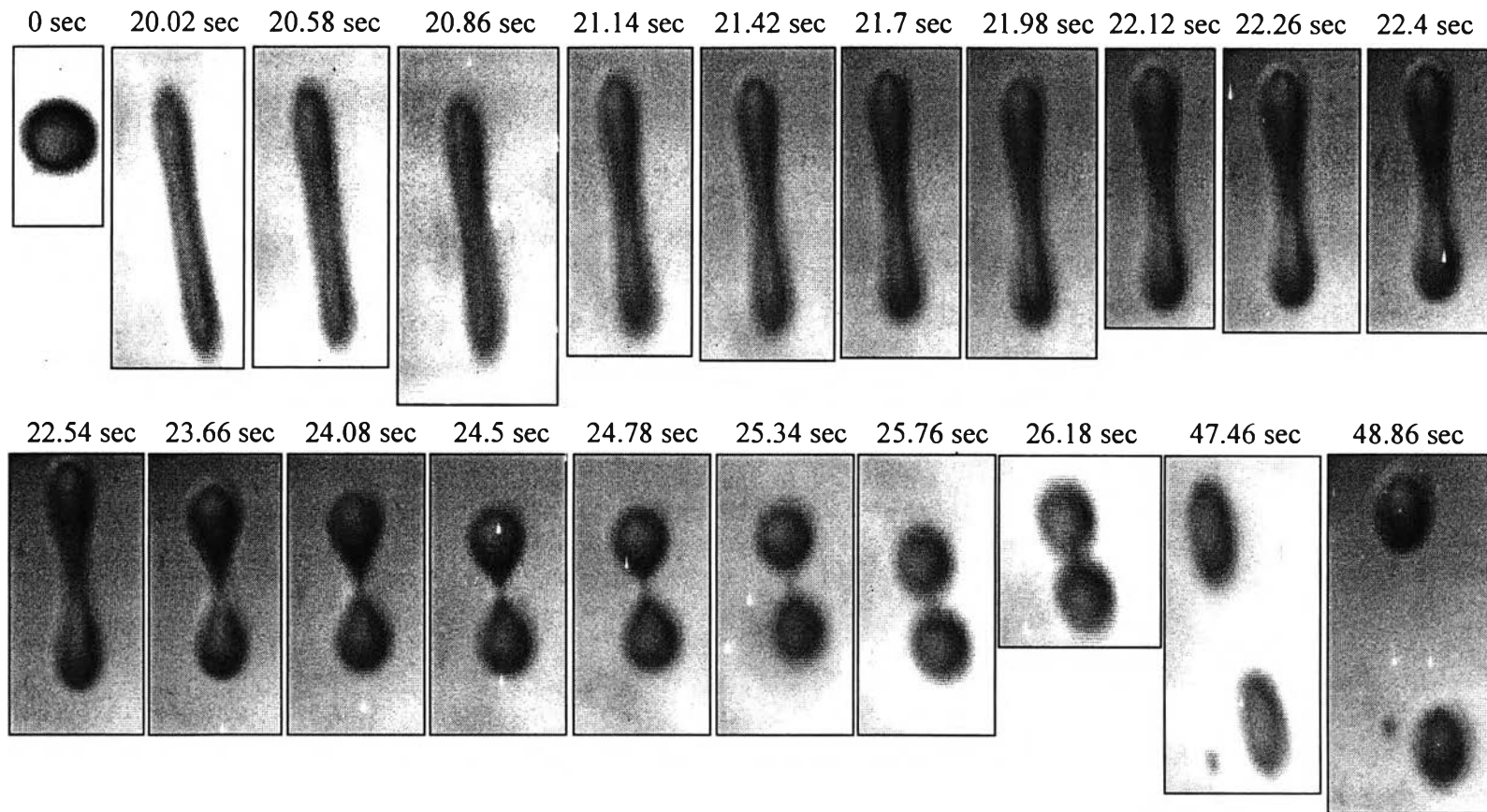
Figure 7 Droplet breakup under shear at strain = 558 %, frequency = 0.05 Hz, G''_r = 0.16, τ_r = 0.029, T = 33 °C, d_o ~ 150 μm and gap 2,200 μm, and at magnification 40x.
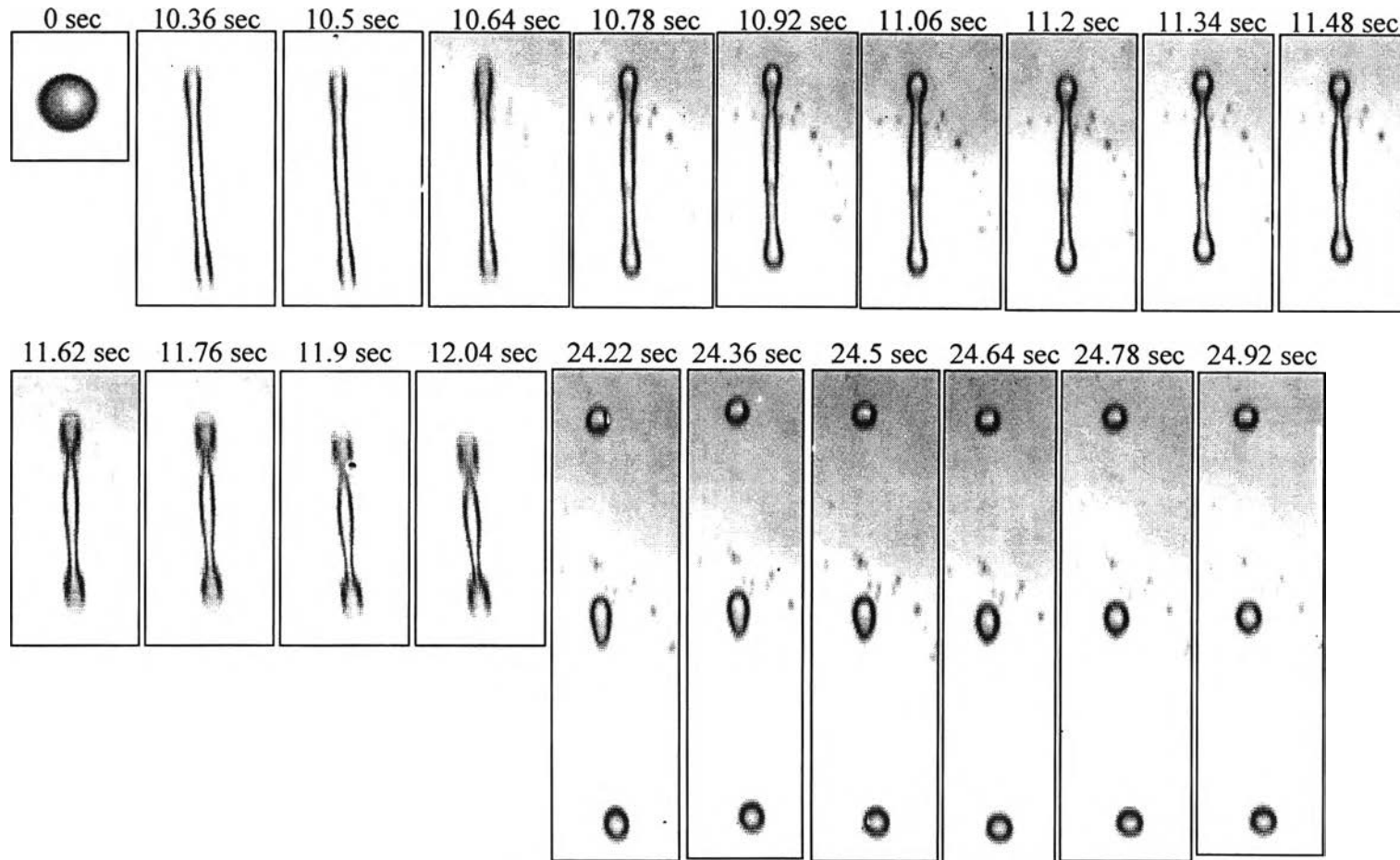
Figure 8 Droplet breakup under shear at strain = 545 %, frequency = 0.1 Hz, G''_r = 0.16, τ_r = 0.0585, T = 67 °C, d_o ~ 150 μm and gap 2,200 μm, and at magnification 40x.

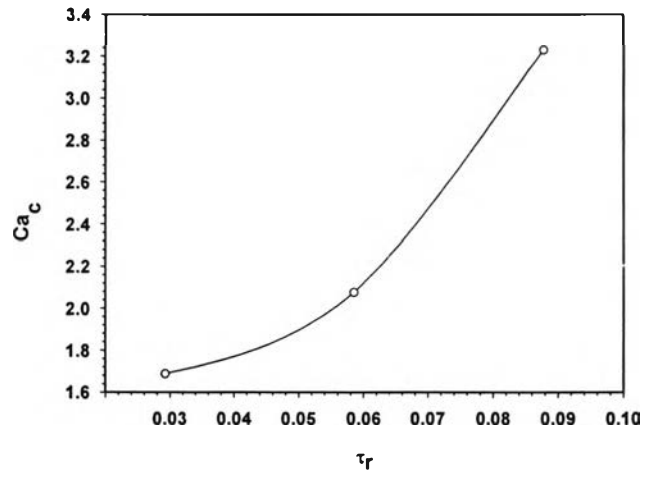**Figure 9** Critical capillary number vs. τ_r of PBd/PDMS at T = 67 °C, G''_r = 0.16 d_o ≈ 150 μm, gap = 2,200 μm: frequency = 0.05 Hz, τ_r = 0.029; frequency = 0.1 Hz, τ_r = 0.0585; frequency = 0.5 Hz, τ_r = 0.08775.